6-23-2006

The Importance of the Strictly Conserved, C-terminal Glycine Residue in Phosphoenolpyruvate Carboxylase for Overall Catalysis: Mutagenesis and Truncation of Gly-961 in the Sorghum C4 Leaf Isoform

Wenxin Xu

Shaheen Ahmed

Hideaki Moriyama
University of Nebraska-Lincoln, hmoriyama2@unl.edu

Raymond Chollet
University of Nebraska-Lincoln, rchollet1@unl.edu

Published in *Journal of Biological Chemistry* 281:25 (June 23, 2006), pp. 17238-17245; doi 10.1074/jbc.M602299200

This research was supported in part by United States National Science Foundation Grant MCB-0130057 (to R. C.) and was published as No. 15,172 in the University of Nebraska Agricultural Research Division journal series.

Submitted March 10, 2006; revised April 18, 2006; published online April 18, 2006.

The Importance of the Strictly Conserved, C-terminal Glycine Residue in Phosphoenolpyruvate Carboxylase for Overall Catalysis: Mutagenesis and Truncation of Gly-961 in the Sorghum C4 Leaf Isoform

Wenxin Xu,[1] Shaheen Ahmed,[1] Hideaki Moriyama,[2] and Raymond Chollet [3]

[1] Department of Biochemistry, [2] Department of Chemistry, and [3] Plant Science Initiative, University of Nebraska, Lincoln, Nebraska 68588-0664
W. Xu and S. Ahmed contributed equally to this project and should be considered as joint first-authors.
Corresponding author — R. Chollet, Department of Biochemistry, University of Nebraska–Lincoln, N246 Beadle Center, Lincoln, Nebraska 68588-0664; tel 402 472-2936; fax 402 472-7842; email rchollet1@unl.edu

Abstract

Phosphoenolpyruvate carboxylase (PEPC) is a "multifaceted," allosteric enzyme involved in C4 acid metabolism in green plants/microalgae and prokaryotes. Before the elucidation of the three-dimensional structures of maize C4 leaf and *Escherichia coli* PEPC, our truncation analysis of the sorghum C4 homologue revealed important roles for the enzyme's C-terminal α-helix and its appended $QNTG^{961}$ tetrapeptide in polypeptide stability and overall catalysis, respectively. Collectively, these functional and structural observations implicate the importance of the PEPC C-terminal tetrapeptide for both catalysis and negative allosteric regulation. We have now more finely dissected this element of PEPC structure-function by modification of the absolutely conserved C-terminal glycine of the sorghum C4 isoform by site-specific mutagenesis (G961(A/V/D)) and truncation (ΔC1/C4). Although the C4 polypeptide failed to accumulate in a PEPC$^-$ strain (XH11) of *E. coli* transformed with the Asp mutant, the other variants were produced at wild-type levels. Although neither of these four mutants displayed an apparent destabilization of the purified PEPC homotetramer, all were compromised catalytically *in vivo* and *in vitro.* Functional complementation of XH11 cells under selective growth conditions was restricted progressively by the Ala, ΔC1 and Val, and ΔC4 modifications. Likewise, steady-state kinetic analysis of the purified mutant enzymes revealed corresponding negative trends in k_{cat} and $k_{cat}/K_{0.5}$ (phosphoenolpyruvate) but not in $K_{0.5}$ or the Hill coefficient. Homology modeling of these sorghum C-terminal variants against the structure of the closely related maize C4 isoform predicted perturbations in active-site molecular cavities and/or ion-pairing with essential, invariant Arg-638. These collective observations reveal that even a modest, neutral alteration of the PEPC C-terminal hydrogen atom side chain is detrimental to enzyme function.

Abbreviations: PEPC (*Ppc*), phosphoenolpyruvate (PEP) carboxylase; CAM, Crassulacean acid metabolism; WT, wild type; Amp, ampicillin; Mops, 3-(*N*-morpholino)propanesulfonic acid; Hepps, *N*-(2-hydroxyethyl)piperazine-*N*′-(3-propanesulfonic acid).

Introduction

Phosphoenolpyruvate carboxylase (PEPC[3]; EC 4.1.1.31) is a ubiquitous cytoplasmic enzyme in vascular plants and is also widely distributed among archaeal, (cyano)bacterial, and unicellular green algal species (1-4) (Figure 1). It catalyzes the irreversible, biotin-independent carboxylation of phosphoenolpyruvate (PEP) in the presence of HCO_3^- and Mg^{2+} (or Mn^{2+}) to yield P_i and oxaloacetate and, thus, is involved intimately in photosynthetic and/or anaplerotic C4 dicarboxylic acid metabolism in these organisms. Overall catalysis is composed of a three-step reaction sequence in which carboxyphosphate and the enolate anion of pyruvate are deployed as key reaction intermediates (1, 2). The former molecular species is subsequently cleaved to P_i and free CO_2 within the active site for β-carboxylation of the enolate anion to oxaloacetate. In the above PEPC-containing organisms the enzyme is most often found as a tetramer of identical, ~95–110-kDa subunits, although notable exceptions to this general pattern exist in the Archaea (3) and green microalgae (4, 5).

Given PEPC's cardinal roles in the photosynthetic assimilation of atmospheric CO_2 by certain green plants (i.e. the so-called C4 and Crassulacean acid metabolism (CAM) species), the C4 isoforms and their eubacterial homologues have been studied extensively during the past two decades by a combination of molecular, biochemical, and structural approaches. As a result, an impressive list of advances in PEPC research has been generated and subsequently reviewed (1, 2, 6-9). Notable among these diverse findings is the realization that (**i**) only the vascular plant enzyme is co-regulated posttranslationally by both opposing, allosteric metabolite effectors and the reversible phosphorylation of a specific Ser residue near its N terminus by a dedicated, ~31-kDa Ser/Thr kinase and opposing heterotrimeric protein phosphatase 2A (1-4, 8), (**ii**) several representative green plant and green algal species encode within their nuclear genomes two divergent, PEPC catalytic subunit types, one of which is most closely related phylogenetically to the eubacterial polypeptide that lacks the N-terminal phosphorylation domain typical of plant PEPC and ends in a C-terminal (R/K)NXG tetrapeptide instead of the plant-invariant QNTG motif (2, 4, 10, 11) (Figure 1), and (**iii**) both the eubacterial (*Escherichia coli*) and green plant (*Zea mays* (maize) C4 isoform) homotetramers are arranged structurally as a "dimer-of-dimers," with each monomer composed of 40 or 41 α-helices, respectively, and only 8 β-strands. The catalytic domain is situated at the C-terminal side of the 8-stranded β-barrel, and the two distinct positive and negative allosteric sites are distanced ~15 and 20 Å, respectively, from this domain (2, 6, 12, 13). Notably, two of the mobile elements within the monomer three-dimensional structure contain residues that contribute to both active site and negative allosteric site interactions. Specifically, mobile loop I is composed of the strictly conserved, Gly-rich GXGXXXXRG motif (1-4, 6, 12). Its invariant Arg residue, situated at position 647, 638, and 587 in the maize and *Sorghum bicolor* (sorghum) C4 isoforms and *E. coli* enzyme, respectively, composes part of the allosteric inhibitor (Asp, L-malate) binding site in the Asp-bound, *E. coli* T-state structure (2, 6, 12). In contrast, in the active, R-state structure of maize C4-PEPC this same basic residue has been translocated ~20 Å to near the catalytic

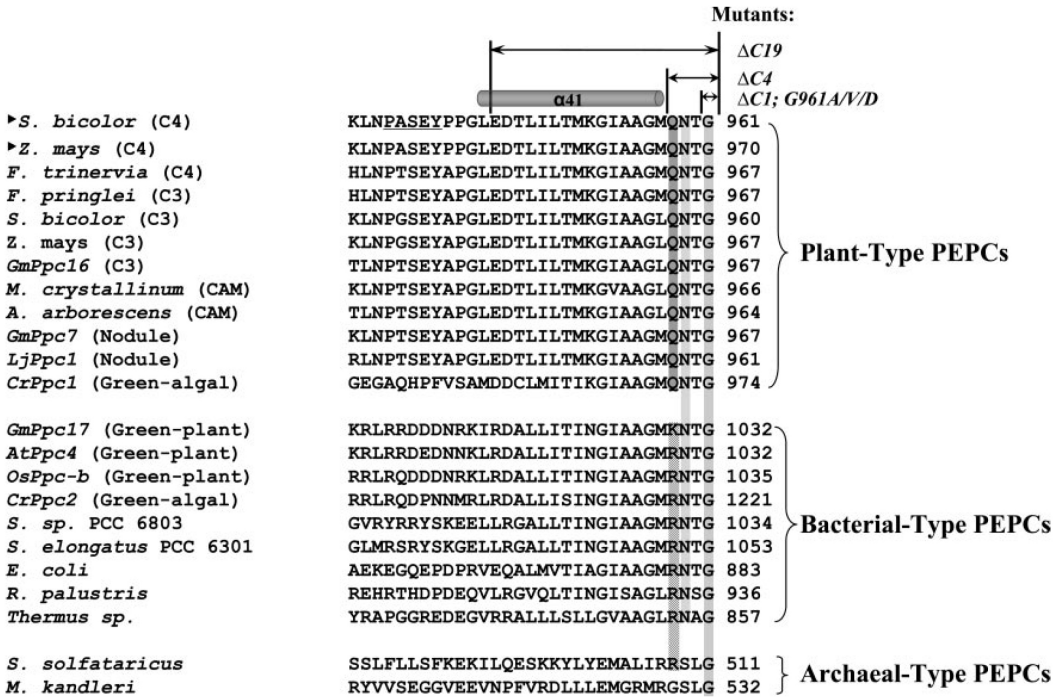

Figure 1. Comparison of the deduced C-terminal amino acid sequence of representative plant-, (cyano)bacterial-, and archaeal-type PEPCs. The source of each sequence was either the NCBI GenBank™ or this study. The abbreviated name and accession number for each PEPC are as follows: *S. bicolor* (C4), *S. bicolor* C4 isoform, CAA45284 and updated in this study; *Z. mays* (C4), *Z. mays* C4 isoform, CAD60555; *F. trinervia* (C4), *Flaveria trinervia* C4 isoform, CAA45504; *F. pringlei* (C3), *Flaveria pringlei* C3-PEPC, CAA45505; S. bicolor (C3), *S. bicolor* C3-isoform, CAA42549; *Z. mays* (C3), *Z. mays* C3-isoform, CAA43709; *GmPpc16* (C3), *Glycine max* PEPC16, C3-PEPC, BAA01560; *M. crystallinum* (CAM), *Mesembryanthemum crystallinum* CAM isoform, CAA32727; *A. arborescens* (CAM), *Aloe arborescens* CAM isoform, E12959; *GmPpc7* (Nodule), *G. max* PEPC7, nodule-enhanced isoform, BAA23419; LjPpc1 (Nodule), *Lotus japonicus* PEPC1, nodule-enhanced isoform, BAC20364; *CrPpc1* (green algal), *Chlamydomonas reinhardtii* PEPC1, AAS01722; *GmPpc17*, *G. max* PEPC17, bacterial-type PEPC, AAS67005; *AtPpc4, Arabidopsis thaliana* PEPC4, bacterial-type PEPC, CAD58727; *OsPpc-b, Oryza sativa* bacterial-type PEPC, BAD44938; *CrPpc2, C. reinhardtii* PEPC2, bacterial-type PEPC, AAS01721; *S. sp.* PCC 6803, *Synechocystis sp.* PCC 6803 PEPC, BAA18393; *S. elongatus* PCC 6301, *Synechococcus elongatus* PCC 6301 PEPC, P06516; *E. coli*, *E. coli* PEPC, P00864; *R. palustris*, *Rhodopseudomonas palustris* PEPC, O32483; *Thermus* sp., *Thermus* sp. PEPC, BAA07723; *S. solfataricus*, *Sulfolobus solfataricus* P2 PEPC, NP–343633; *M. kandleri*, *Methanopyrus kandleri* PEPC, NP–613477. Shading indicates the highly conserved C-terminal tetrapeptide residues in various PEPCs, where *G* is absolutely species-invariant, *N* is conserved in all PEPCs except archaeal-type, *Q* is plant-type PEPCs-only, and *R/K* is conserved in bacterial-type PEPCs-only. The mutants related to this and our previous (16) study were constructed by deleting 19 (ΔC19), 4 (ΔC4), or 1 (ΔC1) residue(s) from the extreme C terminus or by specifically mutating the invariant, C-terminal Gly to Ala, Val, or Asp in the sorghum C4 isoform. Note that (i) the sorghum and maize C4 homologues are 100% identical within these 31 C-terminal residues and 90% identical overall and (ii) the sorghum C4 isoform terminal α-helix 41 extends from Leu-942 to Met-957.

domain, marked by an invariant, essential His (at positions 177, 167, and 138, respectively) within the strictly conserved TXHP motif (Figure 2A). Both of these basic residues have been shown by mutagenesis to be indispensable for overall catalysis by the *E. coli* enzyme (2, 6, 14, 15). Thus, loop I is presumably "trapped" away from the active site upon dicarboxylic acid inhibitor binding to the negative allosteric site by virtue of ionic interaction between this essential Arg side chain and one of the effector's two carboxyl groups. Likewise, in this inhibited T-state the C-terminal tetrapeptide that is appended to the final, buried α-helix is also re-oriented away from near the catalytic domain by H-bonding of its Asn side chain, situated within the N*X*G motif, characteristic of all eubacterial- and plant-type PEPCs (Figure 1), to the allosteric inhibitor (2, 6, 12). Conversely, in the active, R-state structure of the maize C4 isoform this flexible terminal tetrapeptide is found re-positioned to near the active site where it ion-pairs with loop I's invariant and indispensable Arg side chain by virtue of its strictly conserved C-terminal Gly carboxyl (2, 6, 12) (Figures 1 and 2A). Thus, these recent, comparative structural observations implicate the importance of the PEPC C-terminal tetrapeptide for both negative allosteric regulation (Asn) and catalysis (invariant, C-terminal Gly) (2, 6, 12).

Before the elucidation of the active R-state structure of maize C4-PEPC (12, 13), our functional studies of the closely related, sorghum C4 homologue (Figure 1) indicated important roles for the enzyme's C-terminal domain in polypeptide stability and overall catalysis (16). Specifically, mutagenic truncation of the terminal 19 residues (ΔC19 mutant in Figure 1), which deleted the polypeptide's final, hydrophobic α-helix encompassing Leu-942–Met-957 (see α41 in Figure 1) and its adjacent, flexible QNTG^{961} tetrapeptide, resulted in marked reductions in both C4 enzyme accumulation in transformed, PEPC$^-$ *E. coli* cells and *in vivo* and *in vitro* activity. In contrast, when only the plant-invariant, C-terminal tetrapeptide was "trimmed" from the polypeptide (ΔC4 mutant in Figure 1), C4-PEPC levels were restored to near control, wild-type (WT) amounts, but yet maximal catalysis remained compromised by ≥ 99%. Additional studies revealed that the partially purified, ΔC4 mutant protein was unaltered with respect to its ~440-kDa, tetrameric quaternary structure and the phosphorylatability of its N-terminal target Ser-8 residue *in vitro* (16, 17). Clearly, these functional analyses together with the aforementioned structural observations (References 2, 6, and 12; Figure 2A) collectively underscore the importance of this flexible, C-terminal tetrapeptide in PEPC function (and negative allosteric regulation). In the present study we have more finely dissected this element of PEPC structure-function by specific perturbation of the strictly conserved C-terminal Gly residue at position 961 in the sorghum C4 isoform by site-directed mutagenesis and truncation (ΔC1 mutant in Figure 1). The results presented herein highlight the importance of this invariant, simple residue and its minimal, H-atom side chain for maximal *in vivo* activity and in vitro catalytic efficiency of this homotetrameric, allosteric enzyme.

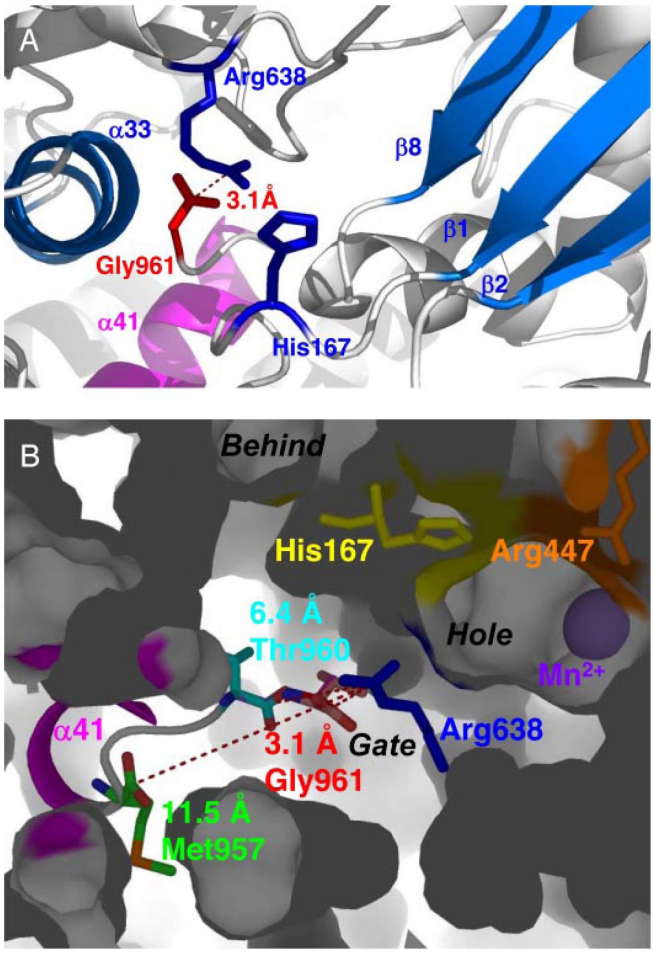

Figure 2. Sorghum C4-PEPC structures modeled from the active maize C4 isoform three-dimensional structure (6, 12, 13). **A**, schematic representation of the active-site domain. β-Strands 1, 2, 8, and α-helix 33 are colored **light blue**, and terminal α-helix 41 is in **magenta**. The invariant (1-4), catalytically essential (14, 15) His-167 and Arg-638 residues (**blue**), and strictly conserved (Figure 1) C-terminal Gly-961 (**red**) are presented with sticks of side chains. The ion pair between the C-terminal Gly carboxyl and Arg-638 guanidino side chain is indicated by red dashes, with a distance of 3.1 Å. **B**, C-terminal truncations (ΔC1/C4) and predicted molecular cavities in the active-site domain. WT and truncated C termini protruding from α-helix 41 (**magenta**) are presented in superimposed models. The C termini are: WT, Gly-961 (**red**); ΔC1, Thr-960 (**sky blue**); ΔC4, Met957 (**light green**). Dashed red lines indicate possible ion-pairing with essential Arg-638, with distances in Å. The approximate locations of the three predicted molecular cavities (Behind essential His-167 (Ala-172—Thr-226); Gate to active site (Arg-447-Arg-638); active-site Hole (Arg-638-C terminus)), described under "Discussion" and Table 2 are noted, as is Arg-447 (**orange**), which corresponds to Arg-456 in β-strand 3 of maize C4-PEPC (12, 13). For reference, the essential Mn^{2+} cofactor (purple sphere) was situated using the 2.6-Å resolution structure of Mn^{2+}- and Asp-bound *E. coli* PEPC (6, 36).

Experimental Procedures

Materials—All buffers and biochemical reagents were obtained from Sigma unless noted otherwise. Liquid [^{14}C]$NaHCO_3$ (55 Ci mol^{-1}) was purchased from MP Biomedicals, Inc. (Irvine, CA), porcine heart L-malate dehydrogenase (~12 units μl-1) was from Roche Applied Science, and rabbit anti-(maize leaf PEPC) IgG was from CHEMICON International, Inc. (Temecula, CA). Prestained Protein-Plus mass standards for SDS-PAGE were from Bio-Rad, and the high molecular weight calibration kit for native PAGE was from Amersham Biosciences.

Construction of the Sorghum C4-Ppc Expression Vector—To obtain stable overexpression of sorghum C4-PEPC in a PEPC$^-$ (*Ppc*$^-$) strain (XH11) of *E. coli* (16, 18, 19), a novel vector was constructed and named *Ppc-P6*. This vector is 4702 base pairs in length and harbors a *ColE1* origin of replication sequence, an ampicillin-resistance gene for antibiotic selection, and a multiple cloning site for convenient cloning, which is flanked by the highly expressed *tac* promoter and strong *txn* transcription terminator to prevent unstable replication (Figure 3). A His_6 tag sequence was inserted between the promoter and the multiple cloning site for affinity purification of the expressed C4-PEPC, and a thrombin cleavage sequence was introduced into the multiple cloning site for potential use. These latter two sequences resulted in a His_6-tagged fusion protein containing 17 extraneous amino acids on its N terminus (Figure 3). However, it should be noted that previous studies have documented that an N-terminal tag domain of 159 extraneous residues has no adverse effects on either the catalytic and allosteric properties or the tetramerization of the maize recombinant C4 isoform (20). Likewise, these observations have been confirmed with the present, much shorter His_6-tagged WT fusion protein relative to our earlier, untagged sorghum recombinant C4-PEPC (see "Results" and Refs. 19 and 21).

A partially re-sequenced and revised WT sorghum C4-*Ppc* open reading frame (Figure 1) or the desired mutant (G961(A/V)) and truncated form (ΔC1/C4) was inserted into the above *Ppc-P6* expression vector between its SmaI and HindIII restriction sites. Briefly, the WT sorghum open reading frame was amplified using primer pair SbWT-SmaI-F (5′-GCATGGCGTCCGAGCGGCACCACTC-3′) and SbWT-HindIII-R (5′-CCCAAGCTTCTAGCCGGTGTTCTGCATGCC-3′) and sorghum leaf total RNA as template following the instructions with the AccuScript™ High-Fidelity RT-PCR kit (Stratagene, La Jolla, CA) and RNeasy Plant mini-kit (Qiagen Inc., Valencia, CA), respectively. After digestion by HindIII and ligation into the *Ppc-P6* expression vector, the WT plasmid DNA in XH11 cells was confirmed by sequencing and restriction enzyme digestion. Subsequently, this WT vector was employed as PCR template to produce the mutant and truncated forms using the *PfuUltra*™ High-Fidelity DNA Polymerase kit (Stratagene) and the following PCR conditions of 2 min at 95 °C, 32 cycles at 98 °C for 25 s, 68 °C for 4 min, and final extension for 10 min at 72 °C. The various primer pairs for these reactions were as follows; the forward primer was Ppc-P6-F (5′-CCGGCTCGTATAATGTGTGGAATTGTGAG-3′), and the reverse primer was SbGA-HindIII-R (5′-CCCAAGCTTCTACGCGGTGTTCTGCATGCC-3′) for G961A, SbGV-HindIII-R (5′-CCCAAGCTTCTAGACGGTGTTCTGCATGCC-3′) for G961V,

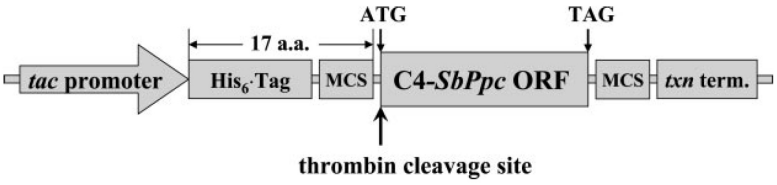

Figure 3. Diagrammatic representation of the novel, *Ppc-P6* vector developed in this study for C4-PEPC overexpression in the PEPC$^-$ *E. coli* strain XH11. Various constructs of the sorghum C4 isoform, driven by the tac promoter, were inserted in the multiple cloning site (*MCS*) between a His_6 tag at the N terminus and a *txn* terminator. The 17 extraneous amino acids (*a.a.*) attached to the tagged N terminus of the PEPC open reading frame (*ORF*) can be trimmed by thrombin to obtain the authentic, untagged *S. bicolor* C4-PEPC if so desired.

SbC1-HindIII-R (5′-CCCAAGCTTCTAGGTGTTCTGCATGCC-3′) for ΔC1, or SbC4-HindIII-R (5′-ACCAAGCTTCTACATGCC-GGCGGCGATACC-3′) for ΔC4, respectively. Untagged mutant G961D was subcloned into the NcoI/HindIII restriction sites of our original, WT pKK311 expression vector (16, 19) using primers pKK311-NcoI-F (5′-AACAATTTCACACAGGAAACAGACCATGGC-3′) and SbGD-HindIII-R (5′-CCCAAGCTTCTAGTC-GGTGTTCTGCATGCC-3′) and pKK233-2 plasmid DNA (18) as template. All mutant and truncated *Ppc* forms were identified and confirmed by sequencing and restriction enzyme digestion. The underlined bases in the above oligonucleotide primers indicate restriction enzyme oligo-sequences.

Culturing of Transformed *E. coli* XH11 Cells—For analysis of *in vivo* functional complementation of the original *Ppc*⁻ strain, each transformed XH11 cell line described above was grown at 30 °C on M9 minimal agar medium (16) supplemented with 50 μg ml^{-1} ampicillin (Amp), 20 μg ml^{-1} Arg, and 0.5% (w/v) succinate. A single colony of each transformant was selected and streaked onto the above-prepared M9 plates, ± succinate, and incubated at 30 °C for up to 2 days.

For cell extraction and subsequent affinity purification of recombinant PEPC, the XH11 cells harboring a specific *Ppc* plasmid DNA were maintained on LB agar medium (16) containing 100 μg ml^{-1} Amp. A single colony of each transformant was selected, inoculated into 5 ml of Terrific Broth medium (16) supplemented with 50 μg ml^{-1} Amp, and incubated overnight with shaking at 37 °C. A 2.5-ml aliquot of this starter culture was added to 1 liter of Terrific Broth medium supplemented with 50 μgml^{-1} Amp and incubated at 37 °C for ~8 h until the A_{600} reached 1.2. The cells were collected by centrifugation, resuspended, and washed once in buffer containing 0.1 M Mops-KOH, pH 7.3, 10 mM $MgCl_2$, 5 mM L-malate (pH adjusted), and the resulting pellets (~6 g) were frozen in liquid N_2 and stored at –80 °C until used.

Extraction and Affinity Purification of Sorghum Recombinant C4-PEPCs—The frozen *E. coli* cells were resuspended in 25 ml of ice-cold extraction buffer containing 0.1 M Mops-KOH, pH 7.3, 10 mM $MgCl_2$, 5 mM L-malate (pH adjusted), 2 mM phenylmethylsulfonyl fluoride, 10 μg ml^{-1} chymostatin, and one tablet of Complete EDTA-free protease inhibitor mixture (Roche Applied Science) per 50 ml of buffer. The resulting suspension was passed twice through a chilled French pressure cell at ~20,000 p.s.i. The crude lysate was centrifuged at 47,800 × g and 4 °C for 30 min, and the supernatant fluid was fractionated at 4 °C with 40-65% saturation ultrapure ammonium sulfate (16). The resulting protein precipitate was dissolved in buffer A (20 mM Tris-HCl, pH 8.0, 5 mM L-malate (pH adjusted), 10% (v/v) glycerol, 10% (v/v) ethylene glycol, 0.5 M ammonium sulfate) containing 2 mM phenylmethylsulfonyl fluoride, 10 μg ml^{-1} chymostatin, and 1 tablet of the above protease inhibitor mixture per 50 ml of buffer and centrifuged at 16,000 × g for 20 min. The clarified solution was applied to a column at 4 °C containing 25 ml of phenyl-Sepharose CL-4B (Sigma) pre-equilibrated with buffer A alone. The column was washed to base line at A_{280} with buffer A, and the bound proteins were eluted with a decreasing, 0.5-0 M ammonium sulfate linear gradient in buffer A (16, 19). The enriched, PEPC-containing fractions that eluted at ~0 M ammonium sulfate were pooled, concentrated, and loaded onto a 2-ml column of His·Bind resin (Novagen, Madison, WI) pre-equilibrated with 20 mM Tris-HCl, pH 7.9, 0.5 M NaCl, 5 mM imidazole, 10% (v/v) glycerol, and the above protease inhibitors. The affinity purification protocol was performed at 4 °C as per the manufacturer's instructions. The fractions eluted by 0.2 M imidazole, pH 7.9, that showed highest PEPC activity were collected, pooled, and concentrated with an iCON™ 20K concentrator (Pierce) to a protein concentration of ~3 mg ml^{-1}. The resulting PEPC preparation was stored in a buffered medium (0.1 M Tris-HCl, pH 7.6, 20% (v/v) glycerol, 10% (v/v) ethylene glycol, 2 mM dithiothreitol, one tablet of protease inhibitor mixture per 50 ml of buffer, 5 μg ml^{-1} chymostatin) at –80 °C until used. The purified proteins were stable for at least 15 days under these conditions.

Measurement of PEPC Activity, Steady-state Kinetic Parameters, and Thermostability—Routine, ΔA_{340}-based spectrophotometric assay of PEPC activity during purification was performed at 25 °C by coupling through exogenous NADH-malate dehydrogenase (4 units) in 50 mM Hepes-KOH, pH 8.0, 1 mM $NaHCO_3$, 10 mM $MgCl_2$, 0.2 mM NADH, ± 5 mM mono(cyclohexylammonium) PEP (21). For more detailed analysis of the purified recombinant proteins, a sensitive, fixed-time radiometric assay was modified from Budde and Chollet (22). The standard reaction mixture contained, in a final volume of 1.0 ml, 50 mM Hepes-KOH, pH 7.3/8.0, 10 mM $MgCl_2$, 2 mM dithiothreitol, 5 units of NADH-malate dehydrogenase, 1 mM NADH, 5 mM $NaH^{14}CO_3$ (0.2-2.0 Ci mol^{-1}), 0, 2, or 5 mM PEP (pH adjusted), and 0.5 μg of PEPC. The reaction at 30 °C was initiated by the addition of PEPC and terminated after 60 s by injection of 0.2 ml of 6 M acetic acid. The acidified assay mixtures were taken to dryness at 90 °C, and PEP-dependent ^{14}C-dpm fixed into acid-stable product was determined by liquid scintillation spectroscopy. One unit of PEPC activity was defined as 1 μmol of oxaloacetate formed (and reduced to L-malate by enzymatic coupling) per min at 30 °C. For steady-state kinetic analysis at pH 7.3 and 30 °C, the concentration range of PEP varied from zero PEP to 10 values between 0.4 and 15.5 mM. All kinetic parameters were determined from the Hill equation fitted to the PEP-dependent experimental data by nonlinear regression analysis (21, 23) using SigmaPlot® 8.0 and Enzyme-Kinetics Module 1.1 (Systat Software Inc., Point Richmond, CA), and k_{cat} values were calculated using a subunit mass of 110,360. Protein concentrations were determined with a sensitive, protein assay kit (Bio-Rad), based on dye binding (24), with crystalline bovine serum albumin as standard.

For comparative analysis of the relative thermostability of the various purified recombinant C4-PEPCs, samples (0.3 mg ml^{-1}) were preincubated in 50 mM Hepps-KOH, pH 8.0, at 35 to 43 °C for up to 30 min (25). Thermo-inactivation was terminated by cooling aliquots on ice for 5 min, and then residual activity was measured radiometrically at 30 °C, pH 8.0, and 5 mM PEP. Given the extremely low activity of the ΔC4-truncated enzyme at 30 °C (see Ref. 16 and "Results"), its heat inactivation was not assessed.

Gel Electrophoresis and Immunoblot Analysis—Non-denaturing PAGE at 4 °C and SDS-PAGE were performed on 7 and 10% separating gels according to Dong et al. (16), Budde and Chollet (22), and Laemmli (26), respectively. The gels were either stained with Coomassie Brilliant Blue or electrotransferred onto polyvinylidene difluoride membranes using a Bio-Rad Mini Trans-Blot apparatus. The membrane was incubated with a 1:5000 (v/v) dilution of rabbit polyclonal antibody raised against maize leaf PEPC, and the antigen-antibody complexes were visualized using ECL Western blotting detection reagents and the accompanying protocol from Amersham Biosciences.

Structural Modeling, Mining, and Model Evaluation—The starting point for homology modeling of the sorghum C4 isoform was the active R-state, 3.0-Å resolution structure of the closely related, maize C4-PEPC (6, 12, 13). These two C4 homologues share 90 and 94% identity and similarity in deduced amino acid sequences, respectively. Homology modeling was performed on the 3D-JIGSAW (27) and SWISS-MODEL (28) web servers. The resulting PDB coordinates were handled using the Change-pdb-chain-id function in the 3D-Dock package (29) for changing chain ID, pdbset in the CCP4 Suite (30) for re-numbering atoms, and BBEdit (Bare Bones Software, Bedford, MA) for general text ed-

iting. The resulting models were evaluated by "Procheck" in the CCP4 Suite. Structural analysis, including local energy minimization, superimpositions, and distances between atoms, was done using Swiss-Pdb Viewer (31). Graphical representations were prepared using PyMOL (DeLano Scientific, San Carlos, CA). Molecular cavities were searched and evaluated using the volume option of the Putative Active Sites with Spheres software (32). Principal component analysis (33) was performed using the statistical computing environment R and the Rweb server of Jean Thioulouse, Université Claude Bernard-Lyon 1, France.

Homology modeling of the sorghum C4 isoform was accomplished successfully based on the maize C4-PEPC structure (PDB code 1jqo (12, 13)). The sorghum three-dimensional model began with residue Ile-26 (maize Ile-35) at the start of α-helix 1 and ended at C-terminal residue Gly-961 (maize Gly-970). This removed the more variable N-terminal domain that contains the phosphorylatable Ser-8 residue (maize Ser-15). The root mean square of distance between the modeled structures and templates were all 0.6 Å in the backbones. This deviation was due to lack of structure in the template, corresponding to sorghum residues Lys-116 —Ser-132 and Pro-751—Ile-760.

Results

Preparation and in Vivo Analysis of the C-terminal Mutant Enzymes—Based on earlier insight into the importance of the PEPC C-terminal tetrapeptide provided by complementary functional and structural analyses (see the Introduction and References 2, 6, 12, and 16), the present study was focused specifically on its terminal Gly, this element's only absolutely conserved residue (Figure 1). The development and use of a novel expression vector for the sorghum C4 isoform (Figure 3) together with our original XH11/*Ppc*$^-$ strain of *E. coli* (16, 19) facilitated the production of various recombinant, His_6-tagged C4 variants in a PEPC$^-$ eubacterial background. Besides the sorghum WT and ΔC4 "reference" enzymes (16), the minimal, H-atom side chain of Gly-961 was replaced conservatively by the two progressively larger, aliphatic hydrocarbon side chains of Ala (G961A) and Val (G961V) containing one or two CH_3 groups, respectively. In addition, the "target" Gly residue was deleted specifically (ΔC1), thereby shortening the 961-residue polypeptide chain by a single amino acid and making the new C-terminal side chain longer and more hydrophilic (Thr-960), or rendered more negatively charged by substitution with the two carboxyl groups of a C-terminal Asp (G961D).

These four new C-terminal mutant forms of sorghum C4-PEPC were first evaluated with respect to their ability to functionally complement *in vivo* the growth phenotype of *Ppc*$^-$ strain XH11 on minimal agar medium. Relative to the WT transformant, all the C-terminal mutants examined in this study were compromised to varying extents with respect to their growth under selective conditions in the absence of the C4 acid succinate. Specifically, the conservative G961A substitution was least affected as compared with WT followed by the G961V and ΔC1 variants (Figure 4). In contrast, neither the ΔC4 nor G961D mutant C4-PEPC supported detectable growth of strain XH11 in the absence of succinate, whereas all six transformants grew equally well in the presence of exogenous C4 acid (Figure 4, data not shown, and Ref. 16). These results indicated that the C4-PEPC variants expressed by these mutants are either essentially inactive (ΔC4, G961D) or not sufficiently active *in vivo* (ΔC1, G961(A/V)) to fully complement the growth phenotype of the XH11/*Ppc*$^-$ strain and/or are insufficiently stable to be accumulated to WT levels in the transformed cells.

To assess to what extent the C4-PEPC polypeptide actually accumulated in these XH11 cells, soluble crude extracts were prepared from liquid cultures grown in rich Terrific Broth medium, resolved by SDS-PAGE, and analyzed by immunoblotting with a polyclonal antibody against the maize leaf enzyme. Whereas four of the five mutant transformants contained essentially WT levels of soluble PEPC protein (Figure 5), the non-conservative G961D variant failed to accumulate detectable, steady-state levels in both the soluble fraction and a total cellular lysate (data not shown). Thus, this non-His_6-tagged, negative charge mutant was not investigated further in this study.

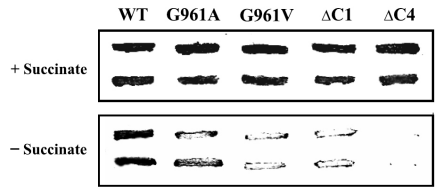

Figure 4. Comparative functional complementation of *E. coli Ppc*$^-$ strain XH11 by wild-type (WT), Gly-961 mutant, and C-terminal truncation forms of sorghum C4-PEPC. Each transformant was grown at 30 °C as a stock culture on an M9 minimal-medium agar plate supplemented with 50μgml^{-1} Amp, 20μgml^{-1} Arg, and 0.5% (w/v) succinate. A single colony of each was subsequently selected and streaked onto a fresh M9 agar plate containing the original levels of Amp and Arg plus (non-selective) or minus (selective) 0.5% (w/v) succinate and incubated for 2 days at 30 °C.

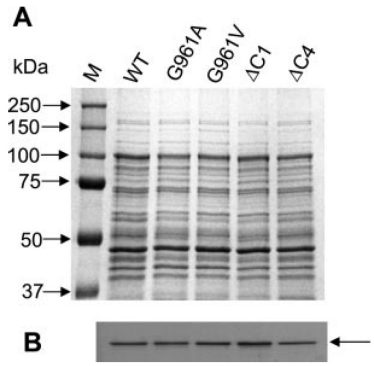

Figure 5. SDS-PAGE and immunoblot analysis of crude soluble extracts from the PEPC$^-$ *E. coli* XH11 cells harboring various sorghum recombinant C4-PEPC constructs. **A**, Coomassie Brilliant Blue-stained 10% SDS-PAGE gel. 5 μg of soluble protein from a centrifuged (~48,000 x g) cell extract was loaded in each lane. The positions of various molecular mass standards (*M*) are indicated at the far left. **B**, corresponding denaturing immunoblot analysis was performed with rabbit anti-(maize leaf PEPC) IgG as described under "Experimental Procedures." The ~110-kDa PEPC polypeptide is indicated by an arrow.

Purification and in Vitro Analysis of the C-Terminal Mutant PEPCs— Given that the four remaining C4-PEPC variants were produced by XH11 cells in WT levels (Figure 5), their varying degrees of functional incompetence *in vivo* (Figure 4) were most likely caused by perturbations in native aggregation state and/or catalytic activity. To explore these possibilities, the soluble His_6-tagged WT and mutant fusion proteins (Figure 3) were purified to electrophoretic homogeneity by sequential ammonium sulfate fractionation, hydrophobic interaction chromatography, and immobilized metal (Ni^{2+}) affinity chromatography (Figure 6A). Analysis of their apparent aggregation state was performed by non-denaturing PAGE at 4 °C and subsequent immunoblotting with the maize C4-PEPC antibodies. Like the WT enzyme, the four purified C-terminal variants migrated to a position in the separating gel consistent with a homotetrameric PEPC, with no immuno-evidence for dimeric and/or monomeric forms (Figure 6B). These findings with the affinity-purified fusion proteins are consistent with those generated previously by size-exclusion fast protein liquid chromatography and native-PAGE analysis of the partially purified, untagged sorghum WT and ΔC4 recombinant enzymes

(16). Clearly, neither modification of the C4-PEPC invariant, C-terminal Gly residue nor its flexible "parent" tetrapeptide causes detectable changes in polypeptide stability, steady-state accumulation, and tetramerization *in vivo,* except for the non-conservative, negative charge G961D substitution.

Based on these observations, the PEPC activity of the four purified variants was next evaluated relative to the control, WT sorghum C4 isoform. For these initial *in vitro* analyses a sensitive ^{14}C-based assay was employed, and PEP-dependent activity was determined at suboptimal but near physiological levels of pH (7.3) and PEP (2 mM) (21). Consistent with the above findings from the *in vivo* functional complementation study (Figure 4), the four C-terminal mutant enzymes also displayed varying degrees of PEPC activity in vitro ranging from ~23% of WT with the modest G961A substitution to only ~0.2% for the ΔC4-truncated form (Figure 6C).

Kinetic Properties of the C-terminal Mutant Enzymes— Given that the above collective findings indicated that all four C-terminal variants were compromised significantly with respect to both *in vivo* and *in vitro* PEPC activity, steady-state kinetic analysis of the purified enzymes became imperative. Because various recombinant C4-PEPC homotetramers have been reported to display varying degrees of cooperative behavior depending on the assay pH and/or specific amino acid modification(s) (13, 21, 23), the ^{14}C-based experimental data were fitted to the Hill equation for calculation of the kinetic parameters $K_{0.5}$ (PEP), V_{max}, and the Hill coefficient (21, 23).

Initial determination of the kinetic properties of the purified WT, His6-tagged fusion protein at pH 7.3 revealed that its respective K0.5 and Vmax values of 1.6 mM and ~36 units mg-1 (Table 1) were similar or superior to those reported previously for the untagged or "trimmed" sorghum and maize recombinant C4 isoforms, respectively (13, 21). This documents that neither this fusion protein's in vivo activity (Figure 4) nor in vitro kinetic constants (Table 1) were affected adversely by its modest 17 amino acid N-terminal extension. These observations agree with earlier related findings with the maize recombinant C4 isoform tagged with 159 extraneous residues on its N terminus (20).

The kinetic properties of the four compromised C-terminal variants were determined next under identical radiometric assay conditions at pH 7.3. Whereas the V_{max} and related k_{cat} values of the three Gly-961-specific modifications ranged from ~25% (G961A) to ~10% (G961V) of WT, those of the ΔC4-truncated form were only ~0.3% (Table 1). These relative kinetic parameters of the purified enzymes essentially mirrored the trends observed in the in vivo functional complementation study (Figure 4). In contrast, the $K_{0.5}$ (PEP) values did not vary markedly from that of the WT enzyme, with the exception of the modest, < 2-fold increase in the ΔC4-truncated form $K_{0.5}$ (Table 1). Consistent with the above kinetic findings, the corresponding decreases in apparent catalytic efficiency or specificity constant ($k_{cat}/K_{0.5}$) of the four C-terminal variants largely reflected those in kcat alone (Table 1) and likewise in *in vivo* functionality (Figure 4). Finally, although there were significant, but ≤ 2-fold decreases in the Hill coefficient (*h*) of the four C-terminal mutants, there was no consistent trend in these changes. For example, the *h* values of the ΔC1/C4 and G961V variants were all ~50% of the WT coefficient (2.4), whereas the respective changes in apparent catalytic efficiency and *in vivo* functional complementation varied markedly between the ΔC4-truncated form and these two other mutants (Table 1, Figure 4).

Thermal Stability of the Purified Gly-961 Mutant Enzymes— One significant experimental variable between the above *in vivo* and *in vitro* activity analyses (Figures 4 and 6C, Table 1) and the related aggregation-state studies (Figure 6B) was temperature, namely 30 versus 4 °C, respectively. Given this difference and the adverse effects on activity measured at 30 °C, it was important to confirm further that the various C-terminal modifications did not grossly perturb the apparent structural stability of the active C4-PEPC homotetramer. To this end, *in vitro* thermal stability experiments were performed with the purified WT and G961 variants (cf. References 25 and 34). Inactivation of the ΔC4-truncated form by elevated temperature was not assessed due to its already

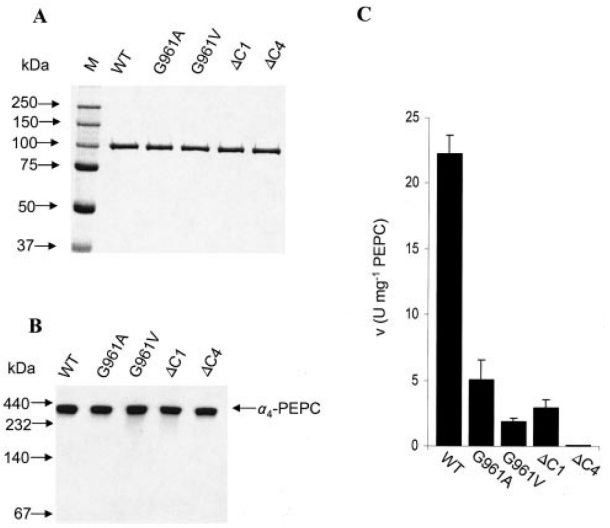

Figure 6. Purity, apparent aggregation state, and activity analysis of purified sorghum recombinant forms of C4-PEPC isolated from transformed XH11 cells. **A**, purified PEPCs (1 μg) were separated by 10% SDS-PAGE, and the gel was stained with Coomassie Brilliant Blue. The positions of various molecular mass standards (M) are indicated at the far left. **B**, purified PEPCs (0.5 μg) were resolved by native PAGE (7% (w/v) separating gel) at 4 °C as described under "Experimental Procedures." Corresponding non-denaturing immunoblot analysis was performed with rabbit anti-(maize leaf PEPC) IgG as described under "Experimental Procedures." The positions of various molecular mass standards are indicated at the far left. The PEPC homotetramer (α4) is indicated by an arrow. C, enzymatic activity of purified PEPCs assayed at suboptimal pH (7.3) and PEP (2 mM). The PEP-dependent activities were measured radiometrically at 30 °C as described under "Experimental Procedures." Values are the mean ± S.D. of 3-4 independent PEPC-preparations, except for the average data (n = 2) for the ΔC4 truncation mutant.

Table 1. Steady-state kinetic analysis of purified sorghum recombinant C4-PEPCs at 30 °C and pH 7.3 All values represent the mean ± S.D. of 3–4 independent PEPC preparations except for the average data (n = 2) for ΔC4.

Enzyme form	V_{max}	$K_{0.5}$	h (Hill coefficient)	k_{cat}	Catalytic efficiency [a]	% WT catalytic efficiency
	Units mg^{-1} PEPC	*mM PEP*		s^{-1}	s^{-1} M^{-1}	
WT	35.9 ± 3.9	1.6 ± 0.2	2.4 ± 0.1	66.0 ± 7.2	4.2 ± 0.1 × 10^4	100
G961A	9.5 ± 1.4	1.8 ± 0.3	1.7 ± 0.1	17.4 ± 2.6	1.0 ± 0.2 × 10^4	24.3 ± 5.5
G961V	3.9 ± 0.1	2.1 ± 0.4	1.3 ± 0.3	7.2 ± 0.2	3.6 ± 0.7 × 10^3	8.5 ± 1.7
ΔC1	5.2 ± 0.5	1.8 ± 0.2	1.2 ± 0.2	9.5 ± 0.9	5.3 ± 1.2 × 10^3	12.6 ± 2.7
ΔC4	0.095	3.0	1.2	0.174	5.9 × 10^1	0.14

[a] $k_{cat}/K_{0.5}$ (or specificity constant).

Table 2. Molecular cavity assessment and principal component analysis. See "Discussion" and Figure 2B

Enzyme form	Cavity volume (no. of probes within 1.8-Å radius)			Projection against the principal component
	Behind His-167 (Ala-172–Thr-226)	Gate (Arg-447–Arg-638)	Hole (Arg-638–C terminus)	
WT	309	565	154	100
G961A	298	559	171	86
G961V	217	609	184	22
ΔC1	245	601	159	62
ΔC4	256	614	178	41

marginal activity at 30 °C (Figure 6C, Table 1, and Reference 16). Neither of the four recombinant enzymes was inactivated by preincubation for 30 min at 35 °C (data not shown). When the preincubation temperature was increased to 40 or 43 °C, they were all progressively inactivated as a function of time, but there were no consistent, major differences between the mutants' thermal inactivation profiles and that of WT C4-PEPC. For example, after a 10-min preincubation at 40 °C, the residual activities measured at 30 °C ranged from 71 (G961V) to 44% (ΔC1), whereas after 2 min at 43 °C they varied from 62 (G961V) to 39% (WT) (data not shown). Likewise, all four recombinant C4-PEPCs were inactivated ≥ 99% after a 10-min pre-incubation at 43 °C. Thus, deleting the invariant, C-terminal Gly residue (ΔC1) or increasing the size of its side chain (G961(A/V)) has no gross effect on apparent homotetramer stability *in vitro* as compared with WT PEPC (Figure 6B, data not shown).

Discussion

This laboratory has had a longstanding interest in the regulatory phosphorylation and structure-function relationships of eukaryotic PEP carboxylase (for review, see Refs. 1, 2, and 8) (4). This cytoplasmic, allosteric enzyme plays a diverse array of important photosynthetic and/or metabolic roles in the varied physiological contexts of green leaves, developing seeds, legume root nodules, and unicellular green algae, to name a few. With respect to its structure-function properties, PEPC has been analyzed in detail since the early 1990s by mutagenesis, x-ray crystallography, and reciprocal C4/C3 enzyme chimeras (for review, see References 1, 2, 6, & 7) (13). These studies have revealed key insights into the homotetramer's "dimer-of-dimers" quaternary structure and the monomer's largely α-helical secondary structure, catalytic domain, and distinct phosphorylation and allosteric effector sites. Although the N-terminal region of the vascular plant polypeptide uniquely harbors the single target Ser residue subject to reversible phosphorylation *in vivo* (1, 2, 8, 19), the more widely conserved C-terminal domain (Figure 1) houses elements important for protein stability, negative allosteric regulation, and maximal overall catalysis (2, 6, 12, 16, 35). Specifically, the C-terminal tetrapeptide of plant- and bacterial-type PEPC contains two conserved residues implicated by x-ray crystallography in allosteric inhibitor binding (Asn) and active site ionic interactions with an essential, invariant Arg side chain (C-terminal Gly) (see the Introduction, Figures 1 and 2A, and References 2, 6, 12, & 35). Prompted by these recent structural observations together with our earlier findings on the importance of the C-terminal, QNTG tetrapeptide for overall catalysis by the sorghum C4 isoform (16), we set out to investigate this strictly conserved Gly residue at the extreme C terminus of sorghum C4-PEPC in the present study.

Perturbation of Gly-961 by either conservative, neutral substitution with Ala (G961A) or Val (G961V) or specific deletion (ΔC1) resulted in neither adverse effects on polypeptide accumulation in a transformed, *Ppc*$^-$/XH11 strain of *E. coli* nor apparent destabilization of the purified homotetramer at below or above ambient temperatures (Figures 5 and 6B and data not shown). Although similar observations were recorded with the more drastic truncation of the entire parent QNTG tetrapeptide (ΔC4), modification of this invariant Gly residue by a negative charge substitution (G961D) resulted in the complete absence of immunologically detectable C4-PEPC in the transformed bacterial cells (data not shown). Evidently, PEPC appears to not tolerate additional negative charge at its extreme C terminus beyond that of the main chain free CO_2^- group.

Despite the aforementioned lack of effect of the G961(A/V) and ΔC1/C4 modifications, these four individual changes led to significant negative perturbation of PEPC activity both *in vivo* and *in vitro.* Functional complementation of XH11 cells under selective, minus succinate growth conditions was restricted progressively by the Ala, ΔC1 and Val, and ΔC4 modifications (Figure 4). Likewise, the effects on *in vitro* activity of the corresponding purified enzymes, assessed at physiological levels of PEP and pH, showed a similarly progressive decline, ranging from ~23% to only ~0.2% of WT C4-PEPC in the G961A and ΔC4 mutants, respectively (Figure 6C). Evidently, even the simplest neutral alteration of the PEPC invariant, C-terminal Gly hydrogen atom side chain to a single CH3 group (i.e. G961A) is detrimental to overall catalysis by the enzyme *in vivo* and *in vitro.* Steady-state kinetic analysis of the purified WT and C-terminal mutant enzyme forms revealed a progressive, significant decrease in the mutant V_{max}, k_{cat}, and specificity ($k_{cat}/K_{0.5}$) constants relative to the WT C4 isoform, with little or no major change in the enzyme $K_{0.5}$ value (Table 1). Thus, specific perturbation of C4-PEPC's strictly conserved C-terminal Gly residue or its parent QNTG tetrapeptide by conservative neutral substitution (G961(A/V)) or truncation (ΔC1/C4) causes up to ~10-1000-fold decreases in overall catalytic efficiency due primarily to changes in k_{cat} alone. These new functional findings provide novel insight into the presumed importance of this enzyme's invariant Gly residue at its extreme C terminus recently derived from the three-dimensional structure of the active R-state form of maize C4-PEPC (see the Introduction and References 2, 6, & 12).

Given the availability of this 3.0-Å resolution structure of the maize C4 isoform, we attempted to evaluate our functional observations in relation to the modeled structure of sorghum C4-PEPC. Notably, the deduced primary structures of these two C4 isoforms are very closely related, bearing a 90 and 94% identity or similarity, respectively, throughout the entire, 961- or 970-residue polypeptide chain and 100% identity within the final 54 C-terminal residues, including all of terminal α-helix 41 (sorghum Leu-942—Met-957) and its appended flexible QNTG tetrapeptide (Figure 1 and data not shown). Homology modeling of the WT sorghum C4-PEPC was in excellent agreement with the maize structure (12, 13) in regard to main-chain folding and, specifically, the active-site domain marked by the C-terminal side of the 8-stranded β-barrel and the invariant catalytically essential His and Arg residues (14, 15) at positions 167 (177) and 638 (647), respectively (sorghum (maize) numbering) (see Figure 2A). Likewise, the strictly conserved C-terminal Gly-961 (-970) carboxyl group was shown to be ion-paired with the guanidino side chain of Arg-638 (-647) situated within 3.1 Å. This active-site Arg, which is embedded in the invariant Gly-rich mo-

tif of mobile loop I, is presumed to partially dissipate the negative charge of the PEP phosphate moiety upon substrate binding to the active R-state enzyme (2, 6, 12). As in WT sorghum C4-PEPC, the distance between this essential Arg side chain and the main-chain CO_2^- group at the extreme C terminus of the G961(A/V) variants is maintained at 3.1 Å. In contrast, this ion pair is compromised in the modeled truncated enzyme forms, with the C-terminal carboxyl of ΔC1 Thr-960 and ΔC4 Met-957 situated 6.4 and 11.5 Å away, respectively, from the guanidino side chain of Arg-638 (Figure 2B).

Finally, we sought to gain additional structural insight into the progressively compromised k_{cat} and specificity constants of the four C-terminal mutant enzyme forms (Table 1) by comparison of putative molecular cavities in modeled structures of the sorghum C4 isoform using the volume option in the Putative Active Sites with Spheres software program (32). From this analysis we found suggestive evidence for alterations in three predicted cavities within the catalytic domain, (i) "behind" essential residue His-167, (ii) by the "gate" to the active site, and (iii) in the "hole" of the active site that houses the essential Mg^{2+} (or Mn^{2+}) cofactor (Figure 2B, Table 2). For the cavity behind His-167 (situated between Ala-172 and Thr-226), all four variants showed a decreased pocket volume. However, only the G961A mutant also displayed an altered shape of this cavity. This concomitant perturbation in cavity shape and volume behind His-167 resulted in a change in the conformation of the residues near this pocket. With respect to the active-site hole cavity between Arg-638 and the extreme C terminus, the G961V mutant enzyme possessed an enlarged pocket, whereas the ΔC4-truncated variant displayed a large positional shift of this cavity toward C-terminal Thr-960 relative to the WT enzyme. The G961A and WT enzyme forms shared a similar shape and size of the gate pocket between Arg-447 and Arg-638, whereas the three other molecular forms had an enlarged gate cavity. To clarify these modeled effects of the mutations, principal component analysis (see "Experimental Procedures") was performed. These three cavity volumes and locations were projected on a principal component axis that explained 93% of the entire variance. The trends in the projected values (Table 2) correlated reasonably well with the experimentally determined perturbations in k_{cat} and catalytic efficiency ($k_{cat}/K_{0.5}$) relative to the WT sorghum enzyme except for the severely compromised ΔC4 variant, which has a large spatial translation of the hole cavity's center due to deletion of the flexible C-terminal QNTG tetrapeptide. In the case of the simplest and most conservative G961A substitution, modest (~4-fold) perturbation of its specificity constant was also enhanced by a concomitant change in the microenvironment around essential His-167. Thus, formation of the requisite reaction intermediates during the 3-step PEPC catalytic sequence (see the Introduction and References 1, 2, & 6) possibly requires more time in these four C-terminal mutant enzymes due to the increased volume of the predicted gate and/or hole cavities, thereby effecting adverse changes in k_{cat} and catalytic efficiency.

In summary, this study provides new functional and structural insight into the invariant nature of the PEPC C-terminal Gly residue and its importance for maximal overall catalysis by the enzyme. As a next step we are presently investigating the conserved proximal Asn at position 959 in sorghum C4-PEPC (see Figure 1) given its presumed role in negative allosteric regulation (2, 6, 12, 35) and the marked perturbation in specificity constant of the "feeble" C-terminal ΔC4 variant relative to the three Gly-961-specific mutants described herein.

Acknowledgments

Shirley Condon is gratefully acknowledged for continued excellence in technical assistance.

References

1. Chollet, R., Vidal, J., and O'Leary, M. H. (1996) *Annu. Rev. Plant Physiol. Plant Mol. Biol.* 47, 273-298
2. Izui, K., Matsumura, H., Furumoto, T., and Kai, Y. (2004) *Annu. Rev. Plant Biol.* 55, 69-84
3. Patel, H. M., Kraszewski, J. L., and Mukhopadhyay, B. (2004) *J. Bacteriol.* 186, 5129-5137
4. Mamedov, T., Moellering, E. R., and Chollet, R. (2005) *Plant J.* 42, 832-843
5. Rivoal, J., Trzos, S., Gage, D. A., Plaxton, W. C., and Turpin, D. H. (2001) *J. Biol. Chem.* 276, 12588-12597
6. Kai, Y., Matsumura, H., and Izui, K. (2003) *Arch. Biochem. Biophys.* 414, 170-179
7. Svensson, P., Bläsing, O. E., and Westhoff, P. (2003) *Arch. Biochem. Biophys.* 414, 180-188
8. Nimmo, H. G. (2003) *Arch. Biochem. Biophys.* 414, 189-196
9. Miyao, M., and Fukayama, H. (2003) *Arch. Biochem. Biophys.* 414, 197-203
10. Sullivan, S., Jenkins, G. I., and Nimmo, H. G. (2004) Plant Physiol. 135, 2078-2087
11. Sánchez, R., Flores, A., and Cejudo, F. J. (2006) *Planta* 223, 901-909
12. Matsumura, H., Xie, Y., Shirakata, S., Inoue, T., Yoshinaga, T., Ueno, Y., Izui, K., and Kai, Y. (2002) *Structure* (Lond) 10, 1721-1730
13. Takahashi-Terada, A., Kotera, M., Ohshima, K., Furumoto, T., Matsumura, H., Kai, Y., and Izui, K. (2005) *J. Biol. Chem.* 280, 11798-11806
14. Yano, M., Terada, K., Umiji, K., and Izui, K. (1995) *J. Biochem.* (Tokyo) 117, 1196-1200
15. Terada, K., and Izui, K. (1991) *Eur. J. Biochem.* 202, 797-803
16. Dong, L., Patil, S., Condon, S. A., Haas, E. J., and Chollet, R. (1999) *Arch. Biochem. Biophys.* 371, 124-128
17. Ermolova, N. V., Cushman, M. A., Taybi, T., Condon, S. A., Cushman, J. C., and Chollet, R. (2003) *Protein Expression Purif.* 29, 123-131
18. Crétin, C., Bakrim, N., Kéryer, E., Santi, S., Lepiniec, L., Vidal, J., and Gadal, P. (1991) *Plant Mol. Biol.* 17, 83-88
19. Wang, Y.-H., Duff, S. M. G., Lepiniec, L., Crétin, C., Sarath, G., Condon, S. A., Vidal, J., Gadal, P., and Chollet, R. (1992) *J. Biol. Chem.* 267, 16759-16762
20. Dong, L.-Y., Hata, S., and Izui, K. (1997) *Biosci. Biotechnol. Biochem.* 61, 545-546
21. Duff, S. M. G., Andreo, C. S., Pacquit, V., Lepiniec, L., Sarath, G., Condon, S. A., Vidal, J., Gadal, P., and Chollet, R. (1995) *Eur. J. Biochem.* 228, 92-95
22. Budde, R. J. A., and Chollet, R. (1986) *Plant Physiol.* 82, 1107-1114
23. Bläsing, O. E., Westhoff, P., and Svensson, P. (2000) *J. Biol. Chem.* 275, 27917-27923
24. Bradford, M. M. (1976) *Anal. Biochem.* 72, 248-254
25. Chen, L.-m., Omiya, T., Hata, S., and Izui, K. (2002) *Plant Cell Physiol.* 43, 159-169
26. Laemmli, U. K. (1970) *Nature* 227, 680-685
27. Bates, P. A., Kelley, L. A., MacCallum, R. M., and Sternberg, M. J. E. (2001) *Proteins Struct. Funct. Genet.* 45, Suppl. 5, 39-46
28. Schwede, T., Kopp, J., Guex, N., and Peitsch, M. C. (2003) *Nucleic Acids Res.* 31, 3381-3385
29. Gabb, H. A., Jackson, R. M., and Sternberg, M. J. E. (1997) *J. Mol. Biol.* 272, 106-120
30. Collaborative Computational Project 4 (1994) *Acta Crystallogr. Sect. D* 50, 760-763
31. Guex, N., and Peitsch, M. C. (1997) *Electrophoresis* 18, 2714-2723
32. Brady, Jr., G. P., and Stouten, P. F. W. (2000) *J. Comput. Aided Mol. Des.* 14, 383-401
33. Sokal, R. R., and Rohlf, F. J. (1981) *Biometry: The Principles and Practice of Statistics in Biological Research,* 2nd Ed., W. H. Freeman and Co., San Francisco
34. Satagopan, S., and Spreitzer, R. J. (2004) *J. Biol. Chem.* 279, 14240-14244
35. Kai, Y., Matsumura, H., Inoue, T., Terada, K., Nagara, Y., Yoshinaga, T., Kihara, A., Tsumura, K., and Izui, K. (1999) *Proc. Natl. Acad. Sci. U.S.A* 96, 823-828
36. Matsumura, H., Terada, M., Shirakata, S., Inoue, T., Yoshinaga, T., Izui, K., and Kai, Y. (1999) *FEBS Lett.* 458, 93-96